Active High Frequency Vibration Rejection in Hard Disk Drives

Seung-Hi Lee, Chung Choo Chung, and Choong Woo Lee

Abstract— **This paper presents an active vibration rejection control technique to reject actuator arm resonance modes using a PZT sensor attached to the actuator arm. A Multi-rate digital implementation is proposed for high frequency active vibration rejection over the sector induced sampling frequency. The vibration control signal can be synchronized with the slow state feedback control input such that the two control signals are summed and applied to the voice coil motor. After obtaining a transfer function from head position to PZT sensor output, a method is proposed on how to design the vibration rejection controller. An application example demonstrates the utility of the proposed active vibration rejection scheme.**

I. Introduction

Actuator resonance modes significantly affect the performance of head positioning servo, limiting bandwidth increase in the design of disk drive servo systems. Also, the actuator resonance modes even cause system instability. The actuator resonance modes even vary accordingly to their gain and frequency variations. Thereby, in the servo design, some design trade-offs are inevitable to attain robustness enough to deal with their gain and frequency variations. Disturbances mostly coming from the disk drive spindle system excite the actuator resonance modes. Although recently introduced fluid dynamic bearing (FDB) spindle system produces much less vibrations than ball bearing one, airflow induced actuator arm and suspension vibrations still remain as a major limiting factor in getting high servo performance. Thus it becomes one of limiting major factors in achieving the required track mis-registration (TMR) budget. To overcome this problem, a phase-stabilized servo controller was developed for dual-stage actuators such that the controller can compensate for windage disturbance by using the structural resonance modes of the microactuator [1].

So far, several techniques has been applied to deal with the resonance mode. Measuring disturbances with accelerometers, one can design feedforward control to reject the effect of external vibrations. In [2], accelerometers attached on the disk drive frame (or PCB) were used to measure the rotational component (centered at the pivot of the actuator) of external vibrations. Measuring actuator arm's vibrations and injecting a counter effect command is also possible. There have been some reports on active vibration control of actuator structural resonance modes. In [3], strain sensors attached on the surface of the suspension were used to measure suspension vibration. In the case of dual-stage actuators, active vibration control using the PZT actuated suspension was reported, where one PZT strip on the suspension is used as a vibration sensor, and the other one as an actuator [4]. Experimental results showed attenuation of both the suspension sway mode and the VCM butterfly mode. However, using the PZT microactuator as an actuator on purpose to reject vibrations may cause undesirable resonance excitation dependent on the control signal applied to the PZT microactuator. An active damping technique was developed for rotary actuators to remove the so-called butterfly mode, which is the major mode in the head mechanical transfer functions and can not be avoided through mechanical design [5], [6]. A strain type sensor was attached to the actuator such that the flexible modes are detected while the rigid body mode is not sensed. The feedback signal was combined with digital servo control signal and fed into the VCM. The butterfly mode could be damped and stiffened. A strain-feedback controller was proposed to overcome the mechanical resonances limiting the servo bandwidth [7]. Application results showed damped primary resonance of VCM actuator.

As illustrated, several techniques can be applied to improve sensitivity in the high frequency region. Among them, active vibration rejection is one of very prospective technique. Although using analog active vibration schemes produced good servo performance improvements, their application in commercial drives requires some calibration work per product. A digital active vibration rejection scheme with sophisticated calibration and control algorithms seems to produce much better results.

This paper presents an active vibration rejection (AVR) control technique to reject actuator arm resonance modes using a PZT sensor attached to the actuator arm. The PZT is used as a sensor only to detect high frequency off-track actuator vibration. The vibration control signal is synchronized with the slow state feedback control input such that the two control signals are summed and applied to the VCM. No control command is to be applied to the PZT. The sampling rate of position error signal (PES) is not affected by the implementation of the proposed scheme. A multi-rate control scheme is introduced in the AVR for the frequencies over the sector induced sampling frequency. Application results are provided to demonstrate the utility of the proposed AVR scheme.

II. An Active Vibration Rejection Scheme

The disk drive actuator with AVR using the PZT sensor output is illustrated in Fig. 1. The AVR scheme using the PZT output is to suppress any resonance modes detected

This work was supported in part by the Advanced Backbone Information and Telecommunication Technology Development Project in Korea.

S.-H. Lee is with Samsung Advanced Institute of Technology, P.O.Box 111, Suwon 440-600, KOREA seunghilee@kornet.net

C. C. Chung and C. W. Lee are with Division of Electrical and Computer Engineering Hanyang University Seoul, 133-791, KOREA, FAX: +82-2-2281-9912, Phone: +82-2-2290-1724 cchung@hanyang.ac.kr, chungwoo73@yahoo.co.kr

via the PZT. It is assumed that the PZT detects off-track vibration modes. Applying the AVR delivers a compensated compound actuator with attenuated resonance excitation (the dotted rectangle in Fig. 1). A VCM controller is to be designed based for the resulting compensated actuator with attenuated resonance modes. Thereby one can attain much higher bandwidth control systems to meet high track density servo requirements. The resulting disk drive actuator control system with the AVR is shown in Fig. 2.

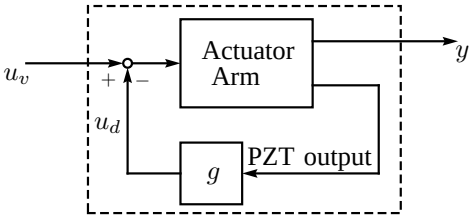

Fig. 1. Actuator with AVR

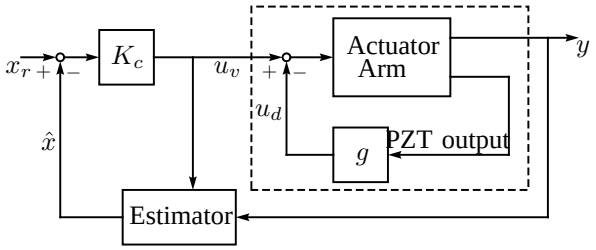

Fig. 2. Disk drive actuator control with AVR

In conventional disk drive the number of sectors and disk rotation speed together limit sampling rate. However, much higher sampling and control rate is needed to reject actuator resonance caused by aerodynamic induced vibrations. For a digital implementation of the AVR scheme, multirate digital implementation is very useful to reject vibrations with frequencies over the sector induced sampling frequency. The VCM control rate is determined by the disk spindle speed and the number of servo wedges on the disk. Thereby the VCM control rate can not be increased enough to cover actuator resonance modes. On the other hand, the PZT sensor output can be measured at a sampling rate much faster without affecting the head position sampling control rate. Also, the VCM control command can be applied to the VCM at a rate much faster than the head position sampling control rate [8]. The vibration control signal is synchronized with the slow VCM control input such that the two control signals are summed and applied to the VCM throughout DAC and the VCM driver. The PES sampling rate is not affected by the implementation of the proposed scheme.

A. AVR Scheme

For the implementation of the proposed AVR scheme, we need a sensor transfer function from the VCM input u_v to the PZT output y_s (Fig. 3). The actuator with a PZT sensor mounted at the hinge of E-block and suspension can be approximately modeled as a compound actuator with VCM and PZT microactuator (MA) (for details, refer to [9]). Then, a sensor transfer function can be developed utilizing the compound actuator transfer function. Here, it should be noted that the PZT sensor output y_s is different from the PZT actuator output y_m.

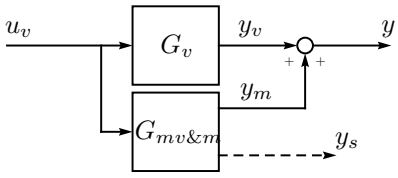

Fig. 3. Block diagram representation of actuator with PZT sensor

Consider a rigid body VCM

$$G_v = \left[\begin{array}{c|c} A_v & B_v \\ \hline C_v & 0 \end{array}\right] \tag{1a}$$

and a VCM with resonances

$$G_{vr} = \left[\begin{array}{c|c} A_{vr} & B_{vr} \\ \hline C_{vr} & 0 \end{array}\right] \tag{1b}$$

where

$$A_v = \begin{bmatrix} 0 & 1 \\ 0 & 0 \end{bmatrix},\ B_v = \begin{bmatrix} 0 \\ l_v K_v / J_v \end{bmatrix},\ C_v = \begin{bmatrix} 1 & 0 \end{bmatrix}.$$

The triplet (A_{vr}, B_{vr}, C_{vr}) is in general obtained from experimental measurements and is assumed to be given. Considering very small PZT sensor's motion and inertia one can describe the compound actuator as

$$G = \left[\begin{array}{c|c} A & B \\ \hline C & 0 \end{array}\right] = \left[\begin{array}{cc|c} A_{vr} & 0 & B_{vr} \\ 0 & A_m & -B_{mv} \\ \hline C_{vr} & C_m & 0 \end{array}\right] \tag{2}$$

with a PZT-suspension model

$$G_{mv\&m} = \left[\begin{array}{c|c} A_m & -B_{mv} \\ \hline C_m & 0 \end{array}\right], \tag{3}$$

where

$$A_m = \begin{bmatrix} 0 & 1 \\ -k_m/J_m & -b_m/J_m \end{bmatrix},\quad B_m = \begin{bmatrix} 0 \\ l_m K_m / J_m \end{bmatrix},$$

$$B_{mv} = B_m\,(1 + l_m/r_m)\,\frac{K_v}{J_v}\frac{J_m}{K_m},\quad C_m = \begin{bmatrix} 1 & 0 \end{bmatrix}.$$

Here, K_v (K_m) is the torque constant of VCM (MA), J_v (J_m) is the inertia of VCM (MA), l_v (l_m) is the length of VCM (MA), k_m and b_m are stiffness and damping factors of MA, r_m is the distance to the MA mass center from the MA pivot.

Here, we approximately represent the PZT sensor to measure actuator arm and PZT resonances by the transfer function

$$G_s = G G_v^+ \tag{4}$$

where

$$G_v^+ = \left[\begin{array}{c|c} A_v & B_v \\ \hline C_v & \epsilon \end{array}\right]^{-1}$$

and ϵ is a very small number which need to be chosen such that $G_v G_v^+$ possibly yields its flattest and smallest frequency response for the low frequencies. The transfer function in (4) with an appropriate value of ϵ then describes the PZT sensor detecting the actuator arm resonance as well as the PZT resonance. The input to the transfer function is u_v, the VCM control input. Thereby after some manipulation (e.g. filtering) of the PZT sensor output y_s, one can obtain an AVR control command

$$u_d = g y_s = g G_s u_v \tag{5}$$

to be injected into the VCM control signal u_v and the resulting signal $u_v + u_d$ is actually applied to the VCM. Accordingly the AVR control signal provides the VCM with a counter-effect signal to reject the actuator arm resonance excitation. The AVR controller g need to have a high-pass (or possibly band-pass) filter shape for appropriate rejection of high frequency actuator arm resonance excitation. In addition, its DC-gain need to be chosen for for matched rigid body frequency responses (between the original and compensated actuator with the AVR). Subsequently, a VCM controller is designed based on the resulting compensated actuator model with the AVR scheme.

Let T_s and T_f be the PES sampling and PZT sensor sampling periods, respectively. Then, the multirate ratio, $R = T_s/T_f$. In this case, the time

$$t = T_s k + T_f i, \quad k = 0, 1, \cdots \quad \text{and} \quad i = 0, 1, \cdots, R-1.$$

In the case when the rate $1/T_s$ can not be increased, one can apply multirate schemes by increasing the rate $1/T_f$ to obtain better results in digital implementation.

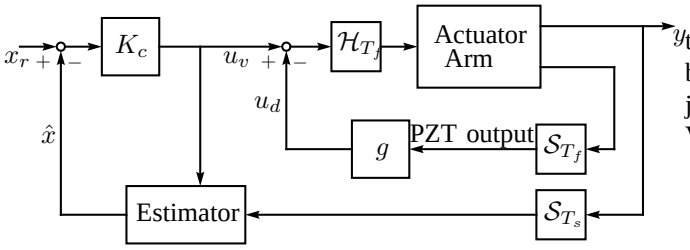

Fig. 4. Multirate digital implementation of disk drive actuator control with AVR

Multirate digital implementation of a disk drive actuator control with AVR is depicted in Fig. 4. Here, K_c is the VCM state feedback controller, $\mathcal{S}_T$ and $\mathcal{H}_T$ are the sampler and holder, respectively, g is the AVR controller transfer function. The PZT sensor output is measured and the vibration rejection control signal u_d is updated every fast sampling period T_f. The VCM control signal u_v and the vibration control signal u_d are summed synchronously and applied to the VCM.

$$u(k,i) = u_v(k,0) + u_d(k,i), \quad i = 0, \cdots, R_u - 1. \tag{6}$$

Here,

$$u_v(k,0) = K_c\left(x_r(k,0) - \hat{x}(k,0)\right)$$

and

$$u_d(k,i) = g y_s(k,i).$$

B. Analysis of the System with AVR

In discrete-time, from the compound actuator system given in (2) the resulting system is described as

$$x(k,i+1) = \Phi x(k,i) + \Gamma u(k,i)$$

where

$$\Phi = e^{AT_f}, \ \Gamma = \int_0^{T_f} e^{A(T_f - t)} dt B.$$

Discrete-time lifting produces

$$x(k+1,0) = \Phi^R x(k,0) + \begin{bmatrix} \Phi^{R-1} & \Phi^{R-2} & \cdots & I \end{bmatrix} \Gamma \begin{bmatrix} u(k,0) \\ u(k,1) \\ \vdots \\ u(k,R-1) \end{bmatrix}. \tag{7}$$

Here, let

$$\tilde{\Gamma} = \begin{bmatrix} \Phi^{R-1} & \Phi^{R-2} & \cdots & I \end{bmatrix} \Gamma,$$

and

$$\tilde{u}(k,0) = \tilde{u}_v(k,0) + \tilde{u}_d(k,0)$$

with

$$\tilde{u}_v(k,0) = \begin{bmatrix} u_v(k,0) \\ u_v(k,0) \\ \vdots \\ u_v(k,0) \end{bmatrix}, \ \tilde{u}_d(k,0) = \begin{bmatrix} u_d(k,0) \\ u_d(k,1) \\ \vdots \\ u_d(k,R-1) \end{bmatrix}.$$

For the closed-loop system to be stable, the state estimator and the state feedback control with the AVR need to be stable. Assuming that the state estimator is stable, we just deal with the zero reference input closed-loop, via the VCM state feedback $u_v(k,0) = -K_c x(k,0)$,

$$x(k+1) = \left(\Phi^R - \sum_{j=0}^{R-1} \Phi^j \Gamma K_c\right) x(k,0) + \tilde{\Gamma} \tilde{u}_d(k,0). \tag{8}$$

Using

$$\Phi_c = e^{AT_s} = \Phi_f^R, \quad \Gamma_c = \sum_{j=0}^{R-1} \Phi^j \Gamma = \int_0^{T_s} e^{A(T_s - t)} dt B$$

we have

$$x(k+1) = \left(\Phi_c - \Gamma_c K_c\right) x(k,0) + \tilde{\Gamma} \tilde{u}_d(k,0). \tag{9}$$

Although the AVR control can be designed independently of the VCM control loop, the resulting system stability seems to be not guaranteed as it can be found in (9).

Let the AVR transfer function from the VCM control $u_v(k,i)$ to the AVR control $\tilde{u}_d(k,i)$

$$g(z) G_s(z) = \left[\begin{array}{c|c} \Phi_s & \Gamma_s \\ \hline C_s & D_s \end{array}\right]. \tag{10}$$

Then, the AVR transfer function from the VCM control $u_v(k,0)$ to the lifted AVR control $\tilde{u}_d(k,0)$ becomes $\left[\begin{array}{c|c} \tilde{\Phi}_s & \tilde{\Gamma}_s \\ \hline \tilde{C}_s & \tilde{D}_s \end{array}\right]$ where

$$\tilde{\Phi}_s = \Phi_s^R,\ \tilde{\Gamma}_s = \Phi_s^{R-1}\Gamma_s + \cdots + \Gamma_s,$$

$$\tilde{C}_s = \begin{bmatrix} C_s \\ C_s\Phi_s \\ \vdots \\ C_s\Phi_s^{R-1} \end{bmatrix},\ \tilde{D}_s = \begin{bmatrix} D_s \\ C_s\Gamma_s + D_s \\ \vdots \\ C_s\left(\Phi_s^{R-2} + \cdots + \Gamma_s\right) + D_s \end{bmatrix}.$$

Then, using (9), it is straightforward to find that the system stability is then determined by the spectrum of

$$\begin{bmatrix} \Phi_c - \Gamma_c K_c - \tilde{\Gamma}\tilde{D}_s K_c & \tilde{\Gamma}\tilde{C}_s \\ -\tilde{\Gamma}_s K_c & \tilde{\Phi}_s \end{bmatrix}.$$

Considering that $(\Phi_s, \Gamma_s, C_s, D_s)$ are designed for an optimal AVR, the state feedback gain K_c should be designed considering the system stability.

As an additional comment to the robustness of the system, it is necessary to provide against sensor aging, malfunctioning that possibly produces very large signal. Many sophisticated calibration and protection algorithms can be applied. Although we do not consider such algorithms here, this is in fact a big advantage of the digital AVR implementation.

III. Application Results

The proposed AVR scheme is applied to a compound actuator with a PZT microactuator from Hutchinson Technology Incorporated. The compound actuator is used because the PZT microactuator can be used as a sensor to measure its vibration. The compound actuator has a 3.6 kHz VCM first resonance and a 6.2 kHz PZT actuator resonance (Fig. 5). The frequency response of the PZT microactuator shows its resonance (Fig. 6). The parameters of the PZT actuator is obtained from the curve-fitting of its experimental frequency response. In this example, the PZT in the compound actuator is to be used as a sensor to detect off-track vibration modes, not an actuator. In practice, however, the PZT in the compound actuator also produces signal for non-off-track vibration modes [10]. Such a sensing problem, that can be resolved with a good sensor, is however beyond the scope of this paper and thus will not be considered here.

The transfer function from the VCM input u_v to the PZT output y_s is shown in Fig. 7. Observe that both VCM and MA resonances are clearly detected in the PZT output. The transfer function from y to PZT sensor output y_s shows a typical (almost linear) shape in Fig. 8.

An AVR controller

$$g = 7.44\frac{s + 6.28 \times 10^3}{s + 3.14 \times 10^5}$$

is designed to have a high-pass filter shape for appropriate rejection of the high frequency actuator arm resonance

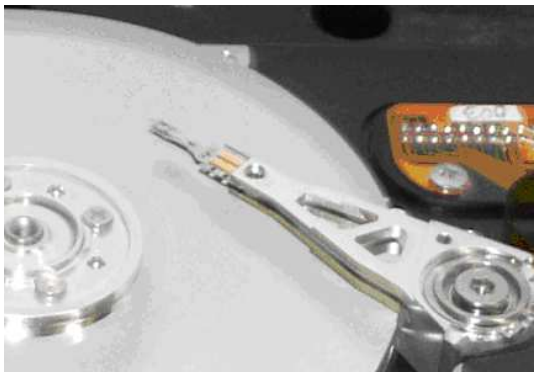

Fig. 5. Compound actuator with PZT microactuator used vibration sensing

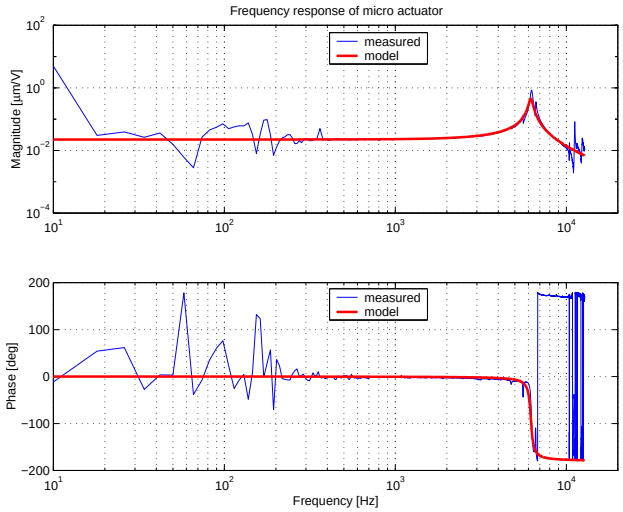

Fig. 6. Experimental frequency response of PZT microactuator

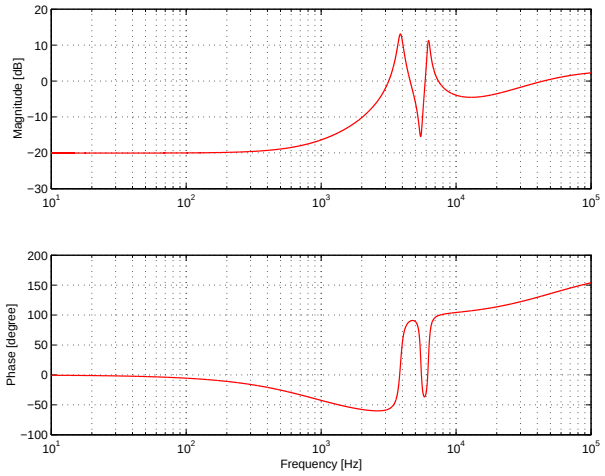

Fig. 7. Transfer function from u_v to PZT sensor output: Both actuator and PZT sensor resonances are detected.

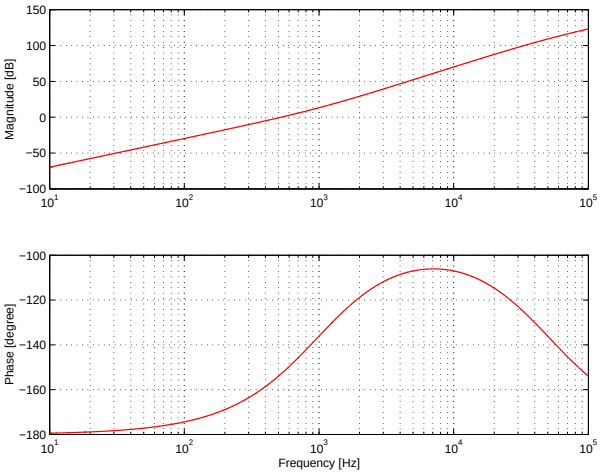

Fig. 8. Transfer function from y to PZT sensor output y_s

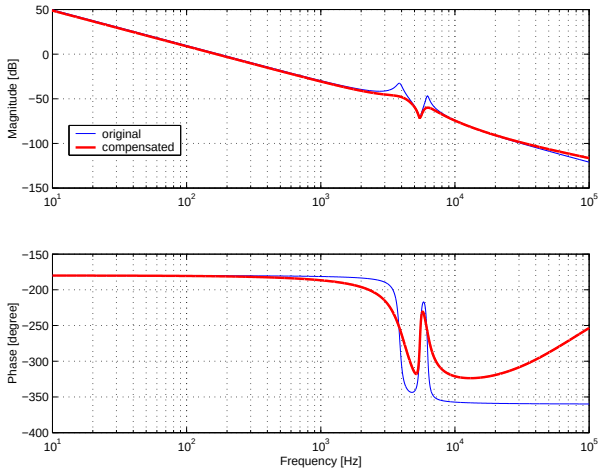

Fig. 10. Compensated plant with AVR: VCM controllers are to be designed based on the compensated actuator model. Thereby higher bandwidth control design is possible.

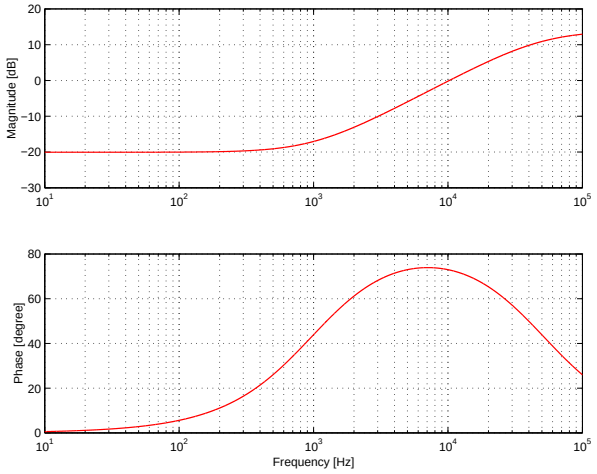

Fig. 9. AVR controller transfer function

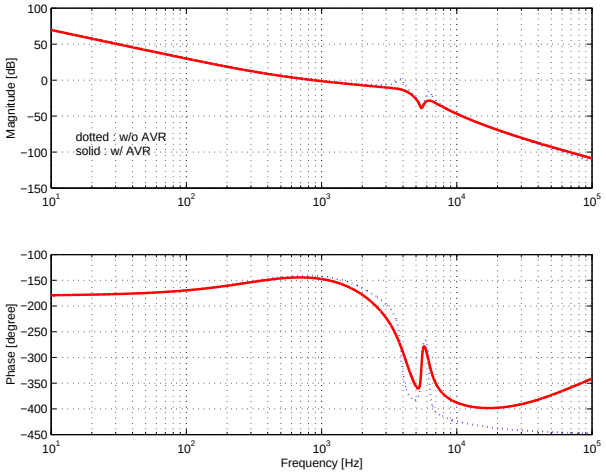

Fig. 11. Loop transfer functions

excitation. As mentioned earlier, its DC-gain is chosen for matched rigid body frequency responses. The AVR controller is discretized via bilinear transformation for digital implementation. Its frequency response is shown in Fig. 9.

Applying the AVR scheme substantially reduces the peak of both VCM and PZT sensor resonances (Fig. 10). Then, a VCM controller is designed based on the resulting compensated actuator model with the AVR scheme. Its effect also appears in the open loop transfer and sensitivity one. Observe the improved open loop via the AVR scheme (Fig. 11). Both actuator and PZT sensor resonances are substantially suppressed via the AVR. Otherwise, the system may become unstable in the presence of disturbances that excite the resonances. Also, observe that the resulting sensitivity function is substantially improved in the high frequency region (Fig. 12). The shape of course varies according to the choice of g, the AVR controller transfer function.

The proposed method was experimentally tested with the PZT microactuator attached to the actuator arm as shown in Fig. 5. For the experiment the servo system is implemented using a 150 MHz TMS320VC33 digital signal processor (DSP) with 16 bit ADCs, and 16 bit DACs. The position of the head is measured using an LDV. A 20 kHz sampling frequency is used for VCM control signal u_v while 80 kHz one is used for AVR control signal u_d. Experimentally measured compensated plant with AVR is plotted with the open loop transfer function of the uncompensated plant illustrated in Fig. 13. Observe that the primary resonance is damped out by about 4 dB. The measured output sensitivity and complementary sensitivity with and without the AVR are shown in Fig. 14.

Although its performance does not come up to our expectation because the PZT sensor also detects non-off-track actuator vibration modes, we observe a good agree-

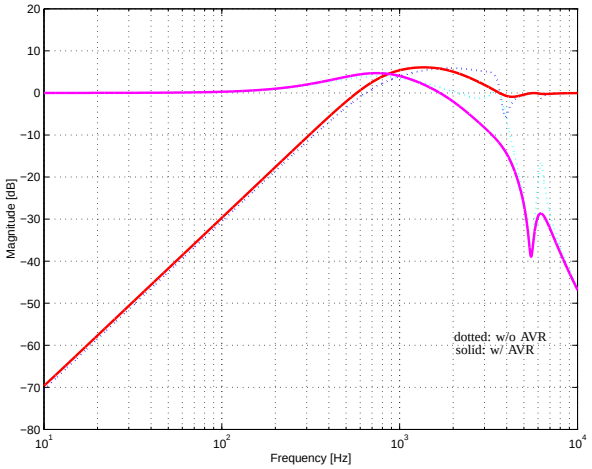

Fig. 12. Output sensitivity and complementary sensitivity with and without AVR: The shape of course varies according to the choice of g, the AVR controller transfer function.

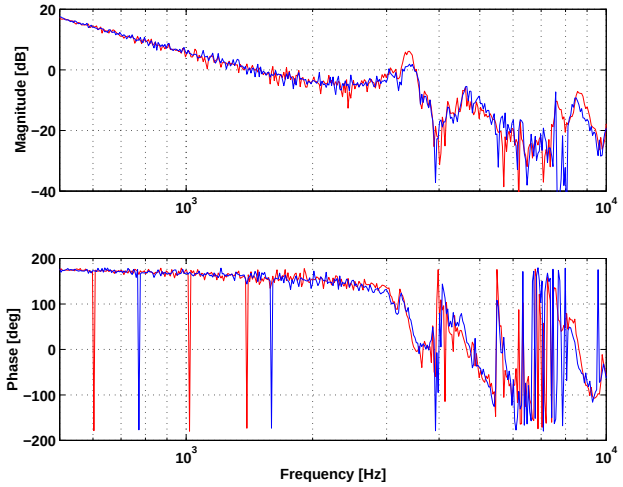

Fig. 13. Open loop transfer functions of the uncompensated plant and compensated one with the AVR

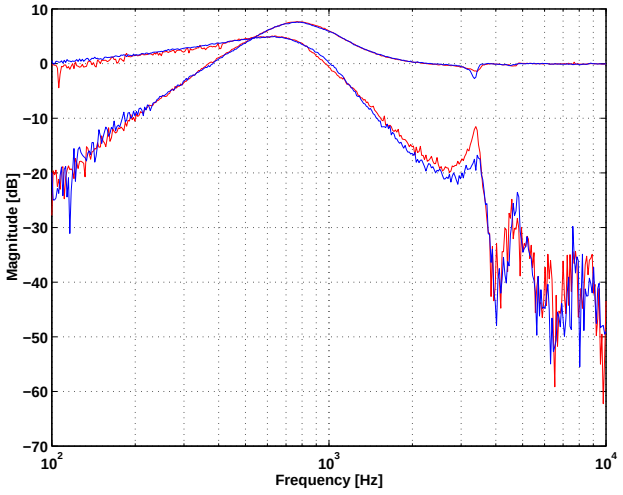

Fig. 14. Measured output sensitivity and complementary sensitivity with and without the AVR

ment between the simulation and experiment results. The application results assures us that applying a better vibration sensor may produce a better result.

The proposed AVR scheme was shown to produces a compensated actuator with substantially reduced resonance modes that can be detected by the PZT sensor. Accordingly, one can design a disk drive actuator controller, based on the resulting compensated actuator model, for a higher bandwidth. This result assures a substantially improved track-follow performance for the frequencies associated with the actuator resonances. Also from the result, it is natural to find the necessity of optimally designed sensors to detect actuator arm resonances.

IV. Conclusions

This paper has presented an active vibration rejection control technique to reject actuator arm resonance modes that can be detected by a PZT sensor attached to the actuator arm. Multirate digital implementation was applied for high frequency active vibration rejection over the sector induced sampling frequency. The vibration control signal was synchronized with the slow state feedback control input such that the two control signals are summed and applied to the voice coil motor. Applying the active vibration rejection scheme produced a compensated plant with substantially reduced resonance peaks. Its effect also appeared in the open loop and sensitivity. The proposed active vibration rejection scheme was shown to be very prospective for high frequency vibration rejection, provided a good vibration sensing scheme is used.

References

[1] M. Kobayashi, S. Nakagawa, and S. Nakamura, “A phase-stabilized servo controller for dual-stage actuators in hard disk drives,” *IEEE Trans. Magnetics*, vol. 39, no. 2, pp. 844–850, 2003.

[2] S.-E. Baek and S.-H. Lee, “Vibration rejection control for disk drives by acceleration feedforward control,” in *Proc. IEEE Conference on Decision and Control*, 1999, pp. 5269–5262.

[3] Y. Huang, M. Banther, P. D. Mathur, and W. C. Messner, “Design and analysis of a high bandwidth disk drive servo system using an instrumented suspension,” *IEEE/ASME Trans. Mechatronics*, vol. 4, no. 2, pp. 196–206, 1999.

[4] Y. Li, R. Horowitz, and R. Evans, “Vibration control of a pzt actuated suspension dual-stage servo system using a pzt sensor,” *IEEE Trans. Magnetics*, vol. 39, no. 2, pp. 932–937, 2003.

[5] F.-Y. Huang, T. Semba, W. Imano, and F. Lee, “Active damping in hdd actuators,” *IEEE Trans. Magnetics*, vol. 37, no. 2, pp. 847–849, 2002.

[6] F. Huang, W. Imaino, and F. Lee, “Active control for stabilizing a servo-controlled actuator system,” *U.S. Patent US6 064 540*, May 2000.

[7] S. Nakagawa, M. Kobayashi, and T. Yamaguchi, “A higher bandwidth servo design with strain feedback control for magnetics disk drives,” in *Proc. American Control Conference*, 2003, pp. 2547–2552.

[8] S.-H. Lee, C. C. Chung, and S.-M. Suh, “Multirate digital control of high track density magnetic disk drives,” *IEEE Trans. Magnetics*, vol. 39, no. 2, pp. 832–837, 2003.

[9] S.-H. Lee and Y.-H. Kim, “Minimum destructive interference design of dual-stage control systems for hard disk drives,” *IEEE Trans. Control Systems Technology*, to appear.

[10] Y. Li, F. Marcassa, R. Horowitz, R. Oboe, and R. Evans, “Track-following control with active vibration damping of a pzt-actuated suspension dual-stage servo system,” *Proc. American Control Conference*, pp. 2553–2559, 2003.